Grounds of VVER-1000 fuel cladding life control

S.N. Pelykh[a,*], M.V. Maksimov [a], V.E. Baskakov [b]

[a]*Odessa National Polytechnic University, Shevchenko av., 1, Odessa, 65044, Ukraine*
[b]*Enertek LLC, P/b 539, Zaporizhzhya reg., Energodar,71504, Ukraine*

CONTENT

Acronyms
Abstract
1. Introduction.
2. CET-method
2.1. Principles of fuel cladding behaviour analysis
2.2. Principles of power flux distribution determination
2.3. CET-method for fuel cladding life estimation
3. Main factors influencing VVER-1000 fuel cladding life
3.1. Determination of the most strained AS
3.2. Choice of the power maneuvering method
3.3. Influence of the fuel cladding corrosion rate
3.4. Determination of VVER-1000 fuel cladding life control methods
4. Optimization of main factors influencing VVER-1000 fuel cladding life
4.1. Determination of the FA distribution
4.2. Calculation of damage in the FE cladding
4.3. The criterion of FA rearrangement efficiency
4.4. The robust model
4.5. Optimization of VVER-1000 FA rearrangements
5. Conclusions
Acknowledgement
References
Figure captions

Acronyms

A-algorithm	advanced power control algorithm	LHR	linear heat rate, W/cm
AO	axial offset, %	LWR	light water reactor
AS	axial segment	M-1, M-2, M-3	power maneuvering methods
COR	adjusting corrosion factor	MATPRO-A	corrosion model
CET	creep energy theory	MCS	Monte Carlo Sampling
CF	reactor capacity factor	NIPC	non-intrusive polynomial chaos
EPRI	corrosion model	NPP	nuclear power plant
FA	fuel assembly	RS	“Reactor Simulator” code
FE	fuel element	SDE	specific dispersion energy, J/m^3
FEMAXI	LWR fuel analysis code	VVER-1000	pressurized-water reactor
KhNPP	Khmelnitskiy NPP		

* Corresponding author. Tel.: +380 66 187 21 45; fax: +380 48 784 38 37.
E-mail address: *1@pelykh.net* ***(S.N. Pelykh).***

Grounds of VVER-1000 fuel cladding life control

S.N. Pelykh[a,*], M.V. Maksimov [a], V.E. Baskakov [b]

[a]*Odessa National Polytechnic University, Shevchenko av., 1, Odessa, 65044, Ukraine*
[b]*Enertek LLC, P/b 539, Zaporizhzhya reg., Energodar,71504, Ukraine*

A VVER-1000 fuel element (FE) cladding failure estimation method based on creep energy theory (CET-method) is physically grounded. Using CET-method, the VVER-1000 regime and fuel design parameters that determine cladding failure conditions are found. It is shown that FE cladding rupture life at normal variable loading operation conditions can be controlled by an optimal assignment of coolant temperature regime and fuel assembly (FA) rearrangement algorithm. Using a FA rearrangement efficiency criterion, it is shown that CET-method allows us to create an automized program-technical complex making control of FE cladding durability and optimization of fuel rearrangements in VVER-1000. *Keywords:* Creep energy theory, Fuel element, Cladding life control, Optimization of fuel, VVER-1000.

Acronyms

A-algorithm	advanced power control algorithm	LHR	linear heat rate, W/cm
AO	axial offset, %	LWR	light water reactor
AS	axial segment	M-1, M-2, M-3	power maneuvering methods
COR	adjusting corrosion factor	MATPRO-A	corrosion model
CET	creep energy theory	MCS	Monte Carlo Sampling
CF	reactor capacity factor	NIPC	non-intrusive polynomial chaos
EPRI	corrosion model	NPP	nuclear power plant
FA	fuel assembly	RS	“Reactor Simulator” code
FE	fuel element	SDE	specific dispersion energy, J/m^3
FEMAXI	LWR fuel analysis code	VVER-1000	pressurized-water reactor
KhNPP	Khmelnitskiy NPP		

2. Introduction

Recently the problem of fuel cladding life control at nuclear power plants (NPP) with VVER-1000 reactors has become actual in Ukraine. First of all, operation of Ukrainian nuclear power units in the variable loading mode is under discussion. The second reason is that existing methods for estimating VVER fuel cladding life under variable loading were worked out near 50 years ago and have become out of date. The VVER-1000 fuel element (FE) cladding total damage parameter is usually estimated by the relative service life of cladding, when steady-state operation and varying duty are considered separately. This approach has the following principal disadvantages [1]:

- disagreement between experimental conditions and real operating environment;
- the physical mechanism (creep) of cladding damage accumulation [2] and the real stress history are not taken into account;
- uncertainty of this cladding life estimate forces us into assumption of an unreasonably high sasety factor [1];
- the cladding failure criterion components depend on VVER-1000 loading conditions, power maneuvering methods, dispositions of regulating units, fuel assembly (FA) rearrangement algorithms, etc.;

* Corresponding author. Tel.: +380 66 187 21 45; fax: +380 48 784 38 37.
E-mail address: *1@pelykh.net* ***(S.N. Pelykh).***

● there is no public data on cladding failure criterion components for all possible VVER-1000 loading conditions, power maneuvering methods, dispositions of regulating units, FA rearrangement algorithms, etc.

The third reason is that, though problems of modernization of control and protection equipment at VVER reactors have been widely discussed for a long time, existing automized program-technical complexes of reactor regulation and protection do not allow us to control life of VVER-1000 FE cladding [3].

At last, the policy of diversification of nuclear fuel supplies was approved in Ukraine recently, hence VVER-1000 core can become mixed, and there is a need to have some universal independent method based on verified codes to compare cladding life under variable loading for fuels of different producers.

The problem of VVER-1000 fuel cladding life control under variable loading consists of several subproblems:

● creating a physically based method of VVER-1000 fuel cladding failure estimation;
● determination of main factors influencing VVER-1000 fuel cladding life;
● working out methods to optimize main factors influencing VVER-1000 fuel cladding life.

2. CET-method

2.1. Principles of fuel cladding behaviour analysis

Though cladding creep test data must have been used to develop and validate the conctitutive models used in the codes to calculate the equivalent creep strains under reactor cyclic loading, difficulty of this problem is explained by the fact that cladding material creep modeling under the conditions corresponding to real operational variable load modes is inconvenient or impossible as such tests can last for years. As a rule, the real FE operational conditions can be simulated in such tests very approximately only, not taking into account all the variety of possible exploitation situations [4].

The light water reactor (LWR) fuel analysis finite element code FEMAXI was used for determination of the evolution of VVER-1000 cladding creep stresses and strains under variable loading in a given power history and coolant conditions. Sintered uranium dioxide was assumed to be the pellet material, while stress-relieved zircaloy-4 was assumed to be the cladding material. The main features of the mathematical model are [5]

● stress/strain analysis is performed using the finite element method with quadrangular elements having four degrees of freedom;
● the creep equation is considered for a multi-axial stress state, the creep strain rate vector is expressed as a vector function of stress and creep hardening parameter, and the creep strain increment vector is found using iterations by the Newton-Raphson method;
● the analysis model includes a two-dimensional axisymmetrical system in which the entire length of the fuel rod is divided into axial segments (ASs), and each AS is divided into concentric ring elements in the radial direction;
● the number of mesh divisions in the radial direction of pellet and cladding is fixed at 10 and 4, respectively. The inner two meshes of cladding are metal phase, and the outer two meshes are oxide layer (ZrO_2). The model used in the code takes into account that the oxide layer mesh and metal mesh change their thickness with the progress of corrosion.
● in the creep model, irradiation creep effects are taken into consideration and cladding creep strain rate $\dot{p}_e$ is expressed with a function of cladding stress, temperature and fast neutron flux. Hence creep strain increases as fast neutron flux, cladding temperature, stress and irradiation time increase;
● the fuel temperature calculation is carried out with the difference between the numerical and analytical solutions not exceeding 0.1%.

2.2. Principles of power flux distribution determination

The amplitude of relative linear heat rate (LHR) jumps at FE ASs occurring when the reactor thermal capacity N increases at power maneuvering, was estimated using the "Reactor Simulator" (RS) code. The main features of the mathematical model are [6]

● power flux distribution is considered using two-group diffusion theory;
● real disposition of regulating units in VVER-1000 is taken into account;
● VVER-1000 constructional and regime parameters are considered;
● distribution of long-lived and stable fission products causing reactor slagging is specified for start moments of real VVER-1000 campaigns;
● the first core state having an equilibrium xenon distribution is calculated for the campaign start moment. Non-equilibrium xenon and samarium distributions are calculated for subsequent states taking into account fuel burnup.

Having calculated relative LHR $k_{v,i,j}$ for AS i of FA j, the corresponding average LHR $< q_{l,i,j} >$ is determined as

$$< q_{l,i,j} >= k_{v,i,j} \cdot < q_l >, \tag{1}$$

where $< q_l >$ is core average LHR, W/cm. If the number of FAs is 163, for N = 100 and 80%: $< q_l >$ = 168.5 and 134.8 W/cm, respectively.

Then $< q_{l,i,j} >$ is represented as

$$< q_{l,i,j} >= q_{l,j,\max} \cdot k_{i,j}, \tag{2}$$

where $q_{l,j,\max}$ is the maximum LHR in FA j; $k_{i,j}$ is the relative power coefficient for AS i of FA j; LHR in the central point of AS i in FA j is set equal to $< q_{l,i,j} >$; LHR values for all other points in each AS are set by linear interpolation of LHR values at the central point of each AS.

2.3. CET-method for fuel cladding life estimation

To predict likelihood of VVER-1000 fuel cladding failure accurately, it is necessary to use a relevant physical model of the fuel cladding failure process during cyclic pressurization. When loading frequency is below 1 Hz, creep governs the entire deformation process in zircaloy-4 cladding [2]. According to creep energy theory (CET), energy spent for FE cladding material destruction is called as specific dispersion energy (SDE) [7]. For the first time, a method of analysis of VVER-1000 FE cladding running time at variable loading based on CET (CET-method) was proposed in [8]. The main features of CET-method are:

● creep is the main mechanism of cladding deformation when VVER-1000 is operated at variable loading;
● creep and destruction processes proceed in common and influence against each other;
● at any moment intensity of failure is estimated by SDE accumulated during creep process by this moment;
● cladding failure criterion components do not depend on VVER-1000 loading conditions, power maneuvering method, disposition of regulating units, FA rearrangement algorithm, etc.

The cladding failure criterion for variable loading is written as:

$$\omega(\tau) = A(\tau)/A_0 = 1;\ A(\tau) = \int_0^{\tau} \sigma_e(\tau)\ \dot{p}_e(\tau)\, d\tau, \tag{3}$$

where $\omega(\tau)$ is cladding material failure parameter; τ is time, s; $A(\tau)$ is SDE, J/m^3; A_0 is SDE at the moment τ_0 that cladding material failure starts, when $\sigma_e(\tau_0) = \sigma_0(\tau_0)$; $\sigma_e(\tau)$, $\dot{p}_e(\tau)$ and $\sigma_0(\tau)$ are, respectively, equivalent stress (Pa), rate of equivalent creep strain (s^{-1}) and yield stress (Pa) for the innermost cladding radial element having the maximum temperature.

According to CET, A_0 does not depend on loading history but, rather, is a characteristic of properties of the cladding material only. When $A(\tau)$ is calculated for different variable loading

cycles, it behaves similarly and in compliance with the experimental results [7]. Generally speaking, A_0 is a probabilistic value having some mean and standard deviation. Under normal VVER-1000 operation conditions, the calculated values of A_0 for zircaloy-4 cladding lie in the range 30−40 MJ/m^3.

Using CET-method, it was found that VVER-1000 regime and FE design parameters were devided into two groups: the parameters that slightly influence the cladding failure moment and the ones that determine it. The second group includes such initial parameters that any one of them gives a change of τ_0 estimation near 2% (or greater) if the initial parameter has been specified at the value assignment interval of 3%. This group consists of cladding diameter and thickness; pellet and pellet centre hole diameters; pellet effective density; FE maximum LHR, initial He pressure and grid spacing; coolant inlet temperature, pressure and velocity, etc. [4]. For example, dependence of cladding SDE on the number of effective days N_{ef}, for pellet hole diameter d_{hole} = 0.140 cm, 0.112 cm and 0.168 cm, is shown in Fig. 1.

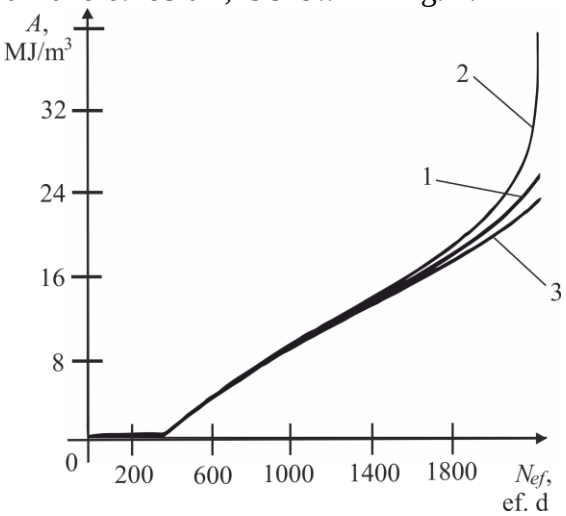

Fig. 1. Dependence of SDE on N_{ef} for d_{hole} : 0.140 cm (1); 0.112 cm (2); 0.168 cm (3).

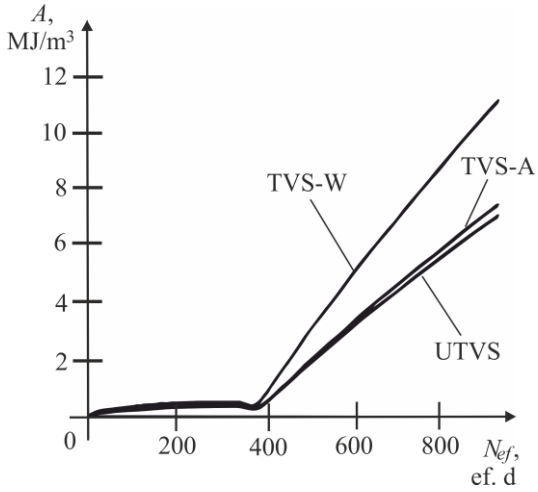

Fig. 2. Dependence of SDE on N_{ef} for UTVS, TVS-A and TVS-W.

The following combined load cycle was studied in [4]: a VVER-1000 works at 100% capacity level within 16 hours, then the reactor is transferred to 75% within 1 h. Further the reactor works at 75% within 6 h, then comes back to 100% within 1 h. But N decreases to 50% within last hour of every fifth day of a week. Further the reactor works during 47 h at 50% and, at last, within last hour of every seventh day N rises to 100%. For the combined cycle, dependence of cladding SDE on $\boldsymbol{N_{ef}}$ for a medium-loading FE of UTVS (serial FA, V-320 project), TVS-A (serial FA, OKBM named after I.I. Aphrikantov) and TVS-W (serial FA, WESTINGHOUSE), is shown in Fig. 2. The maximum SDE value is obtained for FA produced by WESTINGHOUSE, which has no pellet centre hole. The same result was obtained for the stationary regime of VVER-1000. It has been found that cladding running time, expressed in cycles, for the combined cycle decreases from 1925 to 1351 cycles, when FE maximum LHR $q_{l,\max}$ increases from 248 to 298 W/cm. Having done estimation of cladding material failure parameter after 1576 ef. days, it was found that the combined cycle has an advantage in comparison with stationary operation at 100% power level when $q_{l,\max} \leq 273$ W/cm [4].

3. Main factors influencing VVER-1000 fuel cladding life

3.1 Determination of the most strained AS

The assumption was that “the advanced power control algorithm” (A-algorithm) was used during power maneuvering [4]. When using A-algorithm, the 10th regulating group is used only, while the control rods of all the other groups are completely removed from the core. Amplitude of

LHR jumps at ASs occurring when N increases from 80 to 100%, was estimated for the following daily power maneuvering method (M-1): lowering of N from N_1=100% to N_2=90% by injection of boric acid solution within 0.5 h – further lowering of N to N_3=80% due to reactor poisoning within 2.5 h – operation at N_3=80% within 4 h – rising of N to N_1=100% within 2 h – operation at N_1=100% during 15 h. According to M-1, the inlet coolant temperature is kept constant T_{in}=const while N changes in the range N=100–80%, and the initial steam pressure of the secondary coolant circuit changes within the standard range of 58–60 bar.

Using RS it was found that all core cells can be classified into three groups by FA power growth amplitude occurring when N increases from 80 to 100%. In this case, such a 4-year FA transposition algorithm was considered unfavourable for cladding durability: a FA stays in cell 55 (group 2, power growth is 26%) for the 1st year – then it stays in cell 31 (group 1, 28%) for the 2nd year – further it stays in cell 69 (group 2) for the 3rd year – at last, it stays in the central FA (cell 82) position (group 2) for the 4th year. Having calculated the $< q_{l,i,j} > (100\%) / < q_{l,i,j} > (80\%)$ ratio and SDE values for this transposition algorithm, it was found that, on condition that the FE length is divided into 8 equal-length ASs, the 6th (counting from the core bottom) AS limits cladding operation time at daily cycle power maneuvering [1].

3.2 Choice of the power maneuvering method

As one of main tasks at power maneuvering is non-admission of axial power flux xenon waves in the core, therefore, for a power-cycling VVER-1000, it is interesting to consider a cladding life control method on the basis of stabilization of neutron flux axial distribution. The well-known VVER-1000 power control method based on keeping the average coolant temperature constant has such defect as an essential raise of the secondary circuit steam pressure at power lowering, which requires designing of steam generators able to work at an increased pressure. So, the problem of favorable operation conditions for FE claddings is connected to the problems of neutron field axial distribution stability and optimal choice of power maneuvering method. Nonstationary reactor poisoning adds a positive feedback to any neutron flux deviation. Therefore, as influence of the coolant temperature coefficient of reactivity is a fast effect, while poisoning is a slow effect having the same sign as the neutron flux deviation due to this reactivity effect, and strengthening it due to the positive feedback, it can be expected that a correct selection of coolant temperature regime ensures stability of neutron flux axial distribution at power maneuvering**.** Having written the known equation for axial offset (AO) in deviations, using theory of linearization, the criterion of AO stabilization due to the coolant temperature coefficient of reactivity was obtained in [1] as

$$\min \left| \sum_{i=1}^{m} [\delta < T_u > - \delta < T_l >] \right| , \qquad (4)$$

where i is power step number; m is total number of power steps in some direction at reactor power maneuvering.

Use of the criterion allows us to select a coolant temperature regime stabilizing LHR axial distribution at power maneuvering. Let us study the following three VVER-1000 power maneuvering methods: M-1 is the method described earlier (T_{in}=const); M-2 is integrally the same method, but average coolant temperature is kept constant <T>=const; and M-3 is an intermediate method having T_{in} increased by 1 °C only, when N lowers from 100 to 80%. Comparison of these power maneuvering methods was made using RS. Distribution of long-lived and stable fission products was specified for the start of Khmelnitskiy NPP (KhNPP) Unit 2 fifth campaign. Coolant inlet pressure and flow rate were specified equal to 16 MPa and $84 \cdot 10^3$ m^3/h, respectively. When using M-1, coolant inlet temperature was specified at T_{in}=287 °C.

Denoting change of the lowest control rod axial coordinate (%) measured from the core bottom during a power maneuvering as ΔH, the first (M-2a) and second (M-2b) variants of M-2 had the regulating group movement amplitudes ΔH_{2a} =4% and ΔH_{2b} =6%, respectively. For all the methods, reactor power change subject to time was set according to the same time profile: N lowered from N_1=100% to N_2=90% within 0.5 h, under the linear law $dN_{1\text{-}2}/d\tau$=–2%/6 min, at the expense of

boric acid entering. Also for all the methods, N lowered from N_2=90% to N_3=80% within 2.5 h, under the law d$N_{2\text{-}3}$/dτ= –0.4%/6 min, at the expense of reactor poisoning. By means of lowering of concentration of boric acid in the coolant, N stayed constant (80%) during 4 h. Then N increased from N_3=80% to N_1=100% within 2 h, under the law d$N_{3\text{-}1}$/dτ=1.0%/ 6 min, at the expense of pure distillate water entering and synchronous return (under the linear law) of the regulating group to the scheduled position. Setting VVER-1000 operation parameters in accordance with the Shmelev's method [9], for M-1, M-2a, M-2b and M-3, when N changed from 100 to 80%, the change of distribution of the core average LHR was calculated using the RS modelling of non-equilibrium VVER-1000 control, by assignment of: criticality parameter; $T_{in,0}$; dT_{in}/dN; N_1; N_2; N_3; H_0; ΔH; dN/dτ. Calculating the sum according to Eq. (4), the conclusion follows that M-1 gives the most stable AO (2.65**)**, M-2a is least favorable (2.85), while M-3 is an interemediate variant (2.70) [1]. This conclusion was confirmed by calculation of the divergence between instant and equilibrium AOs [1]. The regulating group movement amplitude is the same (4%) for M-1, M-2a and M-3, but the maximum divergence is 1.9% (M-1), 3% (M-2a) and 2.3% (M-3). Therefore, when using the method with $<T>$=const, a greater regulating group movement amplitude is needed to guarantee LHR axial stability, than when using the method with T_{in} = const, if all other conditions are identical [1].

Considering AS 6 and 7, the daily power maneuvering cycle, as well as M-1, M-2a, M-2b and M-3, the changes of core average LHR axial distribution and cladding failure parameter were calculated. Among the regimes with ΔH =4%, M-1 ensuring the most stable AO is characterized by the least $\omega(500\,\mathrm{d})$, while M-2a having the least stable AO is characterized by the greatest $\omega(500\,\mathrm{d})$. The intermediate method M-3 having T_{in} increased by 1 °C only, when N lowers from 100 to 80%, is also characterized by the intermediate values of AO stability and $\omega(500\,\mathrm{d})$. In addition, the second variant of M-2 (M-2b) having $\Delta H_{2\mathrm{b}}$ =6% is characterized by a more stable AO in comparison with M-2a and, for the most strained AS 6, by a greater value of $\omega(500\,\mathrm{d})$. It is also significant that M-1 allows to keep the secondary circuit initial steam pressure within the standard range of 58−60 bar (N=100−80%).

3.3 Influence of the fuel cladding corrosion rate

Growth of the water-side oxide layer of cladding can cause overshoot of permissible limits for the layer outer surface temperature prior to the cladding collapse moment. The corrosion models of EPRI and MATPRO-A [10] have been used for zircaloy cladding corrosion rate estimation when having nucleate boiling flow**.** Under the VVER-1000 conditions, the MATPRO-model estimation of cladding corrosion rate is more conservative than the EPRI-model estimation [1]. Assuming S the oxide layer thickness (m), t is time (days) and that COR is an adjusting corrosion factor $dS/dt = dS/dt\,(1+\mathrm{COR})$, which is added in the FEMAXI code [5], EPRI at COR = − 0.43 gives the calculated cladding oxide layer thickness values which are in compliance with the generalized experimental data for zircaloy-4 [11]. For the most stressed ASs 5–8, the calculated maximum oxide layer outer surface temperature $T_{ox,out}^{\max}$ during the four-year 55–31–69–82 fuel life-time does not exceed the permissible limit temperature $T_{ox,out}^{\lim}$=352 °C [9]. This result was obtained for EPRI at COR = 0; 1; 2, as well as for MATPRO-A at COR = − 0.43; 0; 1; 2. Hence the oxide layer outer surface temperature should not be considered as the limiting factor prior to the cladding collapse moment determined in accordance with the criterion (3). Having calculated SDE using FEMAXI [5], assuming that a FA was transposed in concordance with the 55–31–69–82 four-year algorithm, it was found for AS 6 that the number of calendar daily cycles prior to rapid creep beginning was essentially different at COR = −0.43; 0; 1; and 2. As a result, the rapid creep stage is degenerated at COR = − 0.43 (Fig. 3).

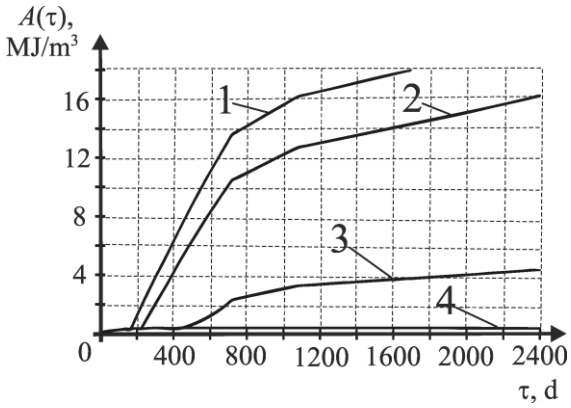

Fig. 3. SDE as a function of time for AS 6: (1, 2, 3, 4) at COR = 2, 1, 0, -0.43, respectively; MATPRO-A.

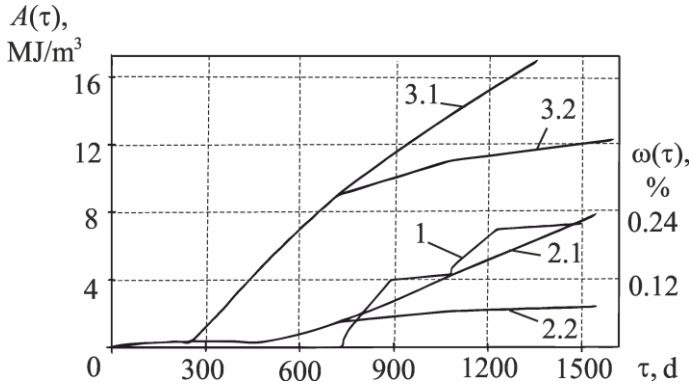

Fig. 4. $\omega(\tau)$ (E-110) and SDE (zircaloy-4) as functions of time: (1) $\omega(\tau)$ according to [13]; (2.1, 2.2) $A(\tau)$ at COR = 0 for the algorithms 55-31-55-55 and 55-31-69-82, respectively; (3.1, 3.2) $A(\tau)$ at COR = 1 for 55-31-55-55 and 55-31-69-82, respectively.

Using EPRI and considering the described method of daily power maneuvering, $T_{ox,out}^{\max}$ during the period of 2400 days and this period averaged cladding inner surface temperature $< T_{clad,in} >$ were calculated for AS 6, and the effect of cladding outer surface corrosion rate (with COR) on cladding SDE increase rate was explained by thermal resistance of oxide thickness and by the corresponding considerable increase in $T_{clad\ ,in}$ [12]. It should be noticed that the metal wall thickness decrease due to oxidation is considered in the calculation of SDE, as effect of cladding waterside corrosion on heat transfer and mechanical behavior of cladding is taken into account in FEMAXI where simultaneous equations of thermal conduction and mechanical deformation are solved [5]. Temperature and $\dot{p}_e(\tau)$ in the innermost cladding radial element increase when outer oxide layer thickness increases. Hence waterside corrosion of cladding is associated with evaluation of SDE through creep rate depending on the thickness of metal wall [12].

Neutron irradiation has a great influence on the zircaloy corrosion behavior. Power maneuvering will alter neutron flux to give a feedback to the corrosion behavior, either positive or negative. Although either temperature or reactivity coefficient is introduced in applying the model, the influence of irradiation on corrosion is not evidently shown in EPRI or MATPRO.

Setting COR = 0 and COR = 1 (MATPRO-A), for 55-31-55-55 and 55-31-69-82 algorithms, the zircaloy-4 cladding behaviour expressed in terms of SDE was compared with the same for E-110 alloy expressed in terms of $\omega(\tau)$ according to [13], where $\omega(\tau)$ was calculated using separate consideration of steady-state operation and varying duty and the fatigue component of $\omega(\tau)$ has an overwhelming size in comparison with the static one (see Fig. 4). So, use of the MATPRO-A corrosion model under VVER-1000 core conditions ensures conservatism of the E-110 cladding durability estimation. The growth rate of $A(\tau)$ depends significantly on the FA rearrangement algorithm. The number of daily cycles prior to the beginning of rapid creep stage decreases significantly when COR (cladding outer surface corrosion rate) increases.

Using CET-method and setting VVER-1000 regime and FA constructional parameters, a calculation study of zircaloy-4 cladding fatigue factor at variable load frequency $\nu << 1$ Hz was carried out. The investigated cladding had an outer diameter and thickness of 9.1 and 0.69 mm, respectively. The microstructure of zircaloy-4 was a stress-relieved state. Using EPRI, AS 6 of a medium-load FE in FA 55 ($q_l^{\max}$=229.2 W/cm at N=100%) was considered (T_{in}=const=287 °C). The variable load cycle 100–80–100% was studied for $\Delta\tau$ =11; 5; 2 h (reactor capacity factor CF=0.9): N lowering from 100 to 80% for 1 h → exploitation at N = 80% for $\Delta\tau$ h → N rising to N=100% for 1 h → exploitation at N = 100% for $\Delta\tau$ h, corresponding to ν=1; 2; 4 cycle/d, respectively(ν << 1 Hz). Calculation of τ_0 according to the condition $\sigma_e(\tau_0) = 0.4 \cdot \sigma_0(\tau_0)$ depending on ν showed that if ν<<1 Hz and CF=idem, then there was no decrease of τ_0 after ν

had increased 4 times, in comparison with the case ν =1 cycle/d, taking into account the estimated error < 0.4% (AS 6). At the same time, when N=100% =const, the calculated τ_0 decreases significantly – see Table 1.

Table 1
Change of cladding failure time depending on ν and CF.

CF		0.9		1
ν, cycle/d	1	2	4	–
τ_0, d	547.6	547.0	549.0	436.6

Hence, the estimation of VVER-1000 FE cladding durability based on CET-method corresponds to the experimental results [2] in principle. Using MATPRO-A and EPRI, for the studied conditions, maximum cladding hoop stress, plastic strain and oxide layer outer surface temperature do not limit cladding durability according to the known restrictions $\sigma_\theta^{\max} \le 250$ MPa, $\varepsilon_{\theta,pl}^{\max} \le 0.5\%$ and $T_{ox,out}^{\max} \le 352$ ºC, respectively.

3.4 Determination of VVER-1000 fuel cladding life control methods

As is shown, operating reactor power history as well as main regime and design parameters included into the second conditional groupe (pellet hole diameter, FE maximum LHR, etc.) influence significantly on fuel cladding durability. At normal operation conditions, VVER-1000 cladding corrosion rate is determined by design constraints for cladding and coolant, and depends slightly on the regime of normal variable loading. But VVER-1000 FE cladding rupture life depends greatly on the coolant temperature regime and the FA rearrangement algorithm. In addition, choice of the regulating group (group 10) disposition influences greatly on AO stabilization efficiency, as this efficiency depends greatly on the distance between neutron-absorbing control rods and fresh FAs. Hence, under normal operation conditions, the following methods of fuel cladding durability control can be considered as main ones [12]:
– choice of FE consrtuction and fuel physical properties, e.g. making fuel pellets of the most strained AS with centre holes.
– choice of the regulating group disposition;
– balance of stationary and variable loading regimes;
– choice of the FA rearrangement algorithm;
– choice of the coolant temperature regime;

Optimization of FE consrtuction and fuel physical properties, as well as optimization of the regulating group disposition are not discussed in detail here, although the corresponding factors can be optimizied in close cooperation with design organizations and producing companies. Optimization of balance of stationary and variable loading regimes can also be excluded here because this factor is determined mainly by an integrated power system. So, in order to ensure fuel cladding durability at VVER-1000 normal operation conditions, the FA rearrangement algorithm and the coolant inlet temperature are to be optimized first of all.

4. Optimization of main factors influencing VVER-1000 fuel cladding life

4.1. Determination of the FA distribution

Optimization of rearrangements of FAs is undertaken for a core segment containing 1/6 of all the FAs, as well as 1/6 of all the regulating units used for power maneuvering. Disposition of the 10th regulating group in case of A-algorithm and the analysed core segment are shown in Fig. 5.

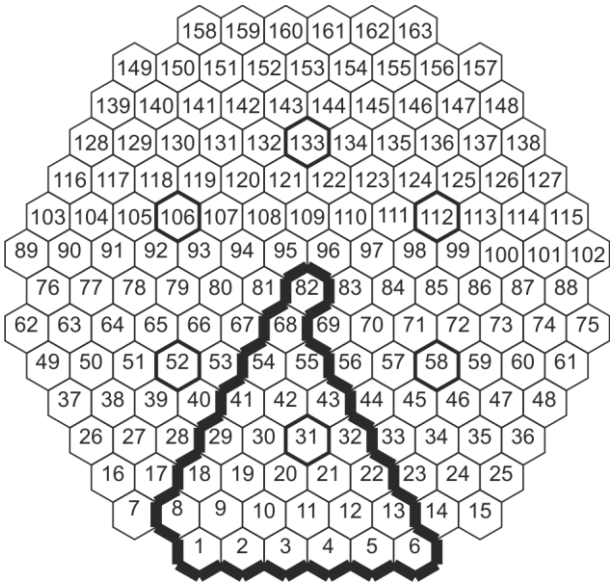

Fig. 5. Disposition of the 10th group: (figure) FA cell number (360 symmetry). The 10-th group cells and the analysed core segment (1/6) borders are in bold.

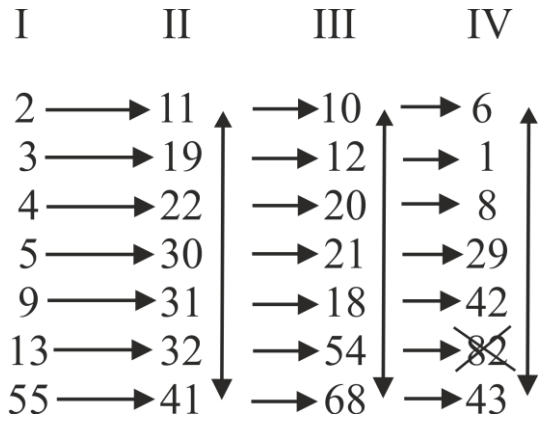

Fig. 6. Transpositions of FAs during rearrangements: (number) FA cell number; (roman numerals I, II, III and IV) 1st, 2nd, 3rd and 4th campaign year, respectively (6 cells for the 4th year FAs).

According to the distribution of long-lived and stable fission products specified for the start of the 5th four-year campaign of KhNPP Unit 2, distribution of FAs in the core segment by campaign year is given in the input data file for the RS code [6]. Having used RS, to establish conditions at the start of the 5th campaign, it was found that there are 7 FAs of each campaign year in the specified core segment. Hence, it can be assumed that at the beginning of each campaign year FAs are placed according to the distribution shown in Fig. 6.

Nowadays two main approaches are used at NPP with VVER-1000 [15]:

- a 4th year FA is placed in the central core cell 82, and 7 core cells are appointed for FAs of each year;
- a 1st or a 2nd year FA is placed in cell 82, and 7 core cells are appointed for FAs of each year, with the exception of 4th year FAs which can be placed in 6 core cells only. In this case cell 82 is not considered when making optimization of FA rearrangements (see Fig. 6).

As the last approach is used in practice mainly, because it gives an optimal fuel utilization to ensure the necessary campaign duration, this approach with 6 cells appointed for 4th year FAs will be considered when making optimization of rearrangements.

4.2. Calculation of damage in the FE cladding

Cladding durability is estimated for the most strained AS 6, taking into account the disposition of regulating units in the A-algorithm case, as well as considering the amplitude of regulating unit movement necessary to stabilize AO at daily power maneuvering with T_{in} = const (method M-1). Changes in SDE during the 4-year campaign (1460 calendar days) were calculated using the MATPRO-A corrosion model by the following procedure:

- Using RS, for the cells shown in Fig. 6, calculation of relative power coefficients $k_{6,j}$ in AS 6 at N=80 and 100%;
- Using FEMAXI, calculation of stress-strain development in FE cladding and fuel burnup;
- Using Eq. (3) and A_0 = 30 MJ/m^3, calculation of ω(1460 d) and burnup B(1460 d) for selected rearrangement algorithms.

If only two core cells (m=2) are used for FAs of each campaign year to optimize their rearrangements in each 1/6 core segment, then the maximum number of possible algorithms is $N_{alg}^{\max} = (2!)^3 = 8$. When we concider all cells in a segment (m=7), $N_{alg}^{\max} = (7!)^3 = 128 \cdot 10^9$. So,

because of a great number of possible variants, when considering a new FA rearrangement algorithm, a random choice of core cells using the MATLAB function "rand" [14] was adopted. To illustrate the method, it was adopted that $N_{alg} = 18$, hence 18 rearrangement algorithms containing 126 different rearrangements were analyzed, where 16 algorithms containing 112 rearrangements were randomly chosen, while two algorithms were practically used at Zaporizhzhya NPP, Unit 5 [15]. These two practical algorithms which were used during campaigns 22 and 23 (algorithms 17 and 18, respectively), as well as two random algorithms (2 and 3) are shown in Table 2 (the rearrangements for the other algorithms are not included in Table 2 in order to shorten its volume).

Table 2
Cladding failure parameter and burnup for algorithms 2, 3, 17 and 18.

Algorithm number (j)	Rearrangement	A, MJ/m^3	$\omega(\tau) = \frac{A}{A_0}$, %	B, MW·d/kg
2	5-30-10-43	1.838	6.127	63.04
	9-11-20-1	1.443	4.81	57.26
	3-22-54-29	1.843	6.143	63.89
	13-19-21-42	2.652	8.84	68.13
	2-31-18	1.209	4.03	47.61
	55-41-12-6	1.955	6.517	59.1
	4-32-68-8	1.368	4.56	57.02
3	9-19-21-8	2.253	7.51	62.49
	5-41-68-43	1.391	4.637	60.47
	55-22-10	2.167	7.223	54.67
	13-11-20-6	1.421	4.737	56.8
	3-30-54-1	1.387	4.623	55.04
	4-32-18-42	1.722	5.74	62.69
	2-31-12-29	1.976	6.587	63.88
17	2-22-12-6	1.463	4.877	54.35
	3-41-29	1.184	3.947	48.8
	4-11-68-43	1.078	3.593	60.63
	5-19-10-8	1.498	4.993	57.18
	9-30-20-1	2.058	6.86	59.39
	13-32-21-42	2.667	8.89	68.23
	55-31-54-18	2.437	8.123	67.45
18	2-22-21-6	1.55	5.167	54.86
	3-41-68	1.18	3.933	48.83
	4-11-29-18	1.159	3.863	60.84
	5-19-20-1	1.449	4.83	54.55
	9-32-12-42	2.586	8.62	67.86
	13-30-10-43	2.551	8.503	67.73
	55-31-54-8	1.982	6.607	61.37

4.3. The criterion of FA rearrangement efficiency

Considering all the FAs used in a rearrangement algorithm j, let's suppose that $\omega_j^{\max}$ is the maximum value of cladding failure parameter, $<\omega>_j$ is the average value of cladding failure parameter; $B_j^{\min}$ is the minimum value of fuel burnup. Let's introduce

$$\omega^{\text{opt}} = \min\{\omega_j^{\max}\};\ \ <\omega>^{\text{opt}} = \min\{<\omega>_j\};\ \ B^{\text{opt}} = \max\{B_j^{\min}\}. \tag{5}$$

Let's accept that $\omega^{\lim}$, $<\omega>^{\lim}$ and $B^{\lim}$ are specified permissible limits for $\omega_j^{\max}$, $<\omega>_j$ and $B_j^{\min}$, respectively. Hence, the permissible values of $\omega_j^{\max}$, $<\omega>_j$ and $B_j^{\min}$ lie in the following ranges:

$$\omega^{\text{opt}} \le \omega_j^{\max} \le \omega^{\lim};\ <\omega>^{\text{opt}} \le <\omega>_j \le <\omega>^{\lim};\ B^{\lim} \le B_j^{\min} \le B^{\text{opt}}. \tag{6}$$

Then we obtain

$$\omega^{\lim,*} \le \omega_j^{\max,*} \le 1;\ <\omega>^{\lim,*} \le <\omega>_j^{*} \le 1;\ B^{\lim,*} \le B_j^{\min,*} \le 1, \tag{7}$$

where

$$\begin{gathered}\omega^{\lim,*} \equiv (1-\omega^{\lim})/(1-\omega^{\text{opt}});\ \omega_j^{\max,*} \equiv (1-\omega_j^{\max})/(1-\omega^{\text{opt}});\ <\omega>^{\lim,*} \equiv (1-<\omega>^{\lim})/(1-<\omega>^{\text{opt}});\\ <\omega>_j^{*} \equiv (1-<\omega>_j)/(1-<\omega>^{\text{opt}});\ B^{\lim,*} \equiv B^{\lim}/B^{\text{opt}};\ B_j^{\min,*} \equiv B_j^{\min}/B^{\text{opt}}.\end{gathered} \tag{8}$$

As $|B^{\lim,*};1|$ can be $>>|\omega^{\lim,*};1|$, from the condition of equal importance of nuclear safety and economy requirements:

$$\omega^{\lim,*} = <\omega>^{\lim,*} = B^{\lim,*}. \tag{9}$$

Hence having some value of $\omega^{\lim}$, the corresponding values of $<\omega>^{\lim}$ and $B^{\lim}$ are defined from the following equations

$$<\omega>^{\lim} = 1-(1-\omega^{\lim})(1-<\omega>^{\text{opt}})/(1-\omega^{\text{opt}});\ B^{\lim} = (1-\omega^{\lim})B^{\text{opt}}/(1-\omega^{\text{opt}}). \tag{10}$$

To compare efficiency *Eff* of different FA rearrangement algorithms, a FA rearrangement algorithm efficiency criterion is proposed:

$$Eff_j = 1 - L_j / L^{\lim}, \tag{11}$$

where

$$L_j = \sqrt{\left(1-\omega_j^{\max,*}\right)^2 + \left(1-<\omega>_j^{*}\right)^2 + \left(1-B_j^{\min,*}\right)^2}, \tag{12}$$

$$L^{\lim} = \sqrt{\left(1-\omega^{\lim,*}\right)^2 + \left(1-<\omega>^{\lim,*}\right)^2 + \left(1-B^{\lim,*}\right)^2}. \tag{13}$$

Using Eqs. (8), (9) and (13)

$$L^{\lim} = \sqrt{3}\left|1-\omega^{\lim,*}\right| = \sqrt{3}\left|\omega^{\lim}-\omega^{\text{opt}}\right|/(1-\omega^{\text{opt}}). \tag{14}$$

The physical meaning of criterion (11) is that

- if any of the dimensionless components ($\omega_j^{\max,*}$, $<\omega>_j^{*}$ or $B_j^{\min,*}$) lies out of the permissible range $[\omega^{\lim,*};1]$, then this component gives a negative contribution to the total efficiency defined by Eq. (11);
- advantage of some algorithm over another is determined on the basis of summation of advantages given by the dimensionless components;
- weight factors can be used in Eq. (9) to give priority to some component.

Using criterion (11) and setting $\omega^{\lim} = 13\%$, *Eff* was calculated for 18 algorithms. Algorithm 2 having the worst *Eff*, the first five algorithms (3, 4, 6, 8, 14) having the greatest values of *Eff*, as well as the practical algorithms (17 and 18) are shown in Table 3.

It can be seen that

- algorithms 3 and 8 are characterizied by both high cladding durability and high burnup, hence all the corresponding dimensionless criterion components are high, so Eff_3 and Eff_8 are highest.
- algorithms 17 and 18 have both cladding durability and burnup worse than the ones of algorithms 3 and 8, so Eff_{17} and Eff_{18} are close to 0.
- algorithm 2 is characterizied by cladding durability close to the same for algorithms 17 and 18, but burnup is considerably lower than the same for these algorithms, and as a result $Eff_2 < 0$.

Table 3
Algorithm efficiency.

j	$\omega_j^{\max}$, %	$<\omega>_j$, %	$B_j^{\min}$, MWd/kg	$\omega_j^{\max,*}$	$<\omega>_j^*$	$B_j^{\min,*}$	Eff_j $\omega^{\lim}=13\%$
2	8.84	5.861	47.61	0.9786	0.999	0.8709	-0.1442
3	7.51	5.865	54.67	0.9929	0.999	1	0.9372
4	6.87	5.796	54.05	0.9998	0.9997	0.9887	0.9008
6	6.847	5.787	53.05	1	0.9998	0.9704	0.741
8	7.017	5.771	54.27	0.9982	1	0.9927	0.9341
14	8.247	5.864	54.07	0.985	0.999	0.989	0.8371
17	8.89	5.898	48.8	0.9781	0.999	0.8926	0.0420
18	8.62	5.932	48.83	0.981	0.9983	0.8932	0.0515

4.4. The robust model

Let us suppose that the calculated maximum LHR in FA j $q_{l,j,\max}$ is the mean of some random variable $q_{l,j,\max}^{\text{rand}}$, i.e.:

$$q_{l,j,\max} \equiv \left\langle q_{l,j,\max}^{\text{rand}} \right\rangle. \tag{15}$$

To take into account VVER-1000 robust operating conditions when making the probabilistic analysis, cladding damage parameter and burnup in the most strained AS 6 are calculated for rearrangements of the best algorithms 3, 4, 6, 8 and 14 (see Table 3) at $\left\langle q_{l,cn,\max}^{\text{rand}} \right\rangle - 10\%$ and $\left\langle q_{l,cn,\max}^{\text{rand}} \right\rangle + 10\%$, where cn is core cell number for the corresponding campaign year, e.g., for algorithm 3 and rearrangement 9-19-21-8: cn = 9, 19, 21 and 8 for 1st, 2nd, 3rd and 4th year, respectively. Hence, use of deterministic criterion (11) allows us to reduce N_{alg} from $N_{alg}=18$ to $N_{alg}=5$.

The efficiency of rearrangement algorithm j is calculated using Eqs. (8) and (11) when

- there are 2 random variables ($\omega_{j,k}^{\text{rand}}$ and $B_{j,k}^{\text{rand}}$) for each pair of algorithm j and rearrangement k;
- $\omega_j^{\max} = \max\{\omega_{j,k}^{\text{rand}}\}$, $<\omega>_j = <\{\omega_{j,k}^{\text{rand}}\}>$, $B_j^{\min} = \min\{B_{j,k}^{\text{rand}}\}$, where $j=1,...,N_{alg}$; $k=1,...,7$.

Hence, we have the total number of input random variables $2\cdot N_{alg}\cdot 7 = 70$, that is 35 rearrangements are described by 70 random variables.

For $k=1,...,7$ and j=3, 4, 6, 8, 14, using three sigma rule (assuming normal distribution), the corresponding means $<\omega_{j,k}^{\text{rand}}>$, $<B_{j,k}^{\text{rand}}>$ and standard deviations $\sigma(\omega_{j,k}^{\text{rand}})$, $\sigma(B_{j,k}^{\text{rand}})$ of random variables $\omega_{j,k}^{\text{rand}}, B_{j,k}^{\text{rand}}$ are calculated. For instance, algorithm 3 − (9-19-21-8 + 5-41-68-43 + 55-22-10 + 13-11-20-6 + 3-30-54-1+ 4-32-18-42 + 2-31-12-29) − is described by the following random values $\tau_{j,p,k}$, where p=1 denotes $\omega_{j,k}^{\text{rand}}$ and p=2 denotes $B_{j,k}^{\text{rand}}$:

$$\tau_{3,1,1} \equiv \omega_{9\text{-}19\text{-}21\text{-}8}^{\text{rand}};\ ...\tau_{3,1,7} \equiv \omega_{2\text{-}31\text{-}12\text{-}29}^{\text{rand}};\ \tau_{3,2,1} \equiv B_{9\text{-}19\text{-}21\text{-}8}^{\text{rand}};\ ...\tau_{3,2,7} \equiv B_{2\text{-}31\text{-}12\text{-}29}^{\text{rand}}.$$

Hence, for rearrangement 9-19-21-8 of algorithm 3, $\tau_{3,1,1}$ and $\tau_{3,2,1}$ are random values described by $\{<\omega_{3,1}^{\text{rand}}>,\ \sigma(\omega_{3,1}^{\text{rand}})\}$ and $\{<B_{3,1}^{\text{rand}}>,\ \sigma(B_{3,1}^{\text{rand}})\}$, respectively.

As we have 70 random variables, non-intrusive polynomial chaos (NIPC) methods [16] are not computationally attractive in comparison with Monte Carlo Sampling (MCS) methods. To use the

MCS method, a set of normally distributed random variables $\tau_{j,p,k}$ is obtained substituting the means and standard deviations of $\omega_{j,k}^{\text{rand}}$ and $B_{j,k}^{\text{rand}}$ into the MATLAB function "normrnd" [14], and the efficiency of algorithm j is found using Eq. (11) in the form:

$$Eff_j = f\left(\theta_{j,1,1}, \theta_{j,1,2}, \theta_{j,2,1}\right), \tag{16}$$

where $j = 1,...,N_{alg}$;

$\theta_{j,1,1} = \max\{\tau_{j,1,1},...,\tau_{j,1,7}\}$; $\theta_{j,1,2} = <\{\tau_{j,1,1},...,\tau_{j,1,7}\}>$; $\theta_{j,2,1} = \min\{\tau_{j,2,1},...,\tau_{j,2,7}\}$.

4.5. Optimization of VVER-1000 FA rearrangements

Thus, the efficiency of algorithm j is calculated using Eq. (16). For the case of uncertain conditions, $\omega^{\text{opt}}, <\omega>^{\text{opt}}, B^{\text{opt}}$ and L^{lim} can not be set as for the deterministic case (see Eq. 5 and Table 4).

Table 4
Difference between the deterministic and robust cases.

Deterministic case			Robust case			
$\omega^{\text{lim}} = 13\%$						
ω^{opt}	$<\omega>^{\text{opt}}$	B^{opt}	MCS	ω^{opt}	$<\omega>^{\text{opt}}$	B^{opt}
6.847	5.771	54.67	1	8.1212	6.79261	55.2311
$<\omega>^{\text{lim}} = 1-(1-\omega^{\text{lim}})(1-<\omega>^{\text{opt}})/(1-\omega^{\text{opt}}) = 0.12;$			10	10.6683	7.93351	55.6857
$B^{\text{lim}} = (1-\omega^{\text{lim}})B^{\text{opt}}/(1-\omega^{\text{opt}}) = 51.06;$			100	9.9501	7.44926	53.8346
$L^{\text{lim}} = \sqrt{3}\left\|\omega^{\text{lim}} - \omega^{\text{opt}}\right\|/(1-\omega^{\text{opt}}) = 0.1144;$			$<\omega>^{\text{lim}}, B^{\text{lim}}, L^{\text{lim}}, \omega^{\text{lim},*}$ are variable on MCS.			
$\omega^{\text{lim},*} \equiv (1-\omega^{\text{lim}})/(1-\omega^{\text{opt}}) = 0.9339.$						

It should be noted that if N_{alg} increases, then ω^{opt} decreases. On the contrary, when the number of core cells used for optimization increases, ω^{opt} increases also. The trade-off between the mean value of Eff_j and its standard deviation, as estimated using MCS, for the best five FA transposition algorithms shown in Table 3, as well as for the simplest robust optimization of FA rearrangements taking into account only two core cells appointed for each year, is shown in Fig. 7.

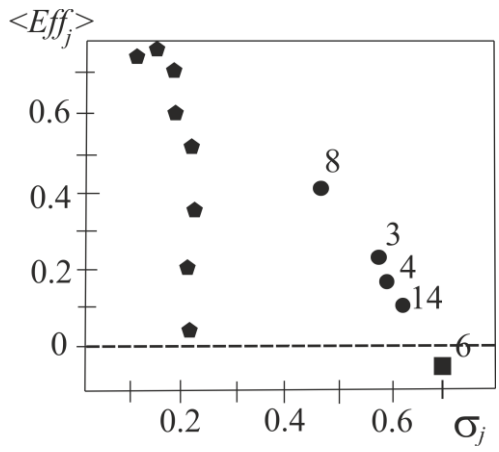

Fig. 7. Mean efficiency and standard deviation for ω^{lim}=13% in the robust case: (number) algorithm number for optimization with 7 cells per year (excluding year 4), A_0=30 MJ/m^3; (pentagon) random algorithm for optimization with 2 cells per year, A_0=40 MJ/m^3.

As shown in Table 3, algorithm 3 had the largest efficiency in the deterministic case, while Fig. 7 shows that in the robust case algorithm 8 is most efficient. This can be explained by the fact that $\omega_3^{\max} \approx 7.5\%$, while $\omega_8^{\max} \approx 7\%$. As dependence of SDE on LHR is nonlinear and SDE depends greatly on FA rearrangement history, in the robust case this difference $\omega_3^{\max} - \omega_8^{\max} = 0.5\%$ turned to be sufficient to obtain a greater mean efficiency for algorithm 8 in comparison with algorithm 3. In addition, algorithm 3 has a greater standard deviation than algorithm 8, and thus there is no trade-off between these two options. Both algorithms dominate all the other options, having both higher mean efficiencies and smaller standard deviations.

5. Conclusions

1. The VVER-1000 FE cladding failure estimation method based on CET is physically grounded because it takes into account influence of real reactor operating environment, stress history as well as the physical mechanism (creep) of cladding damage accumulation.
2. Having found the VVER-1000 regime and fuel design parameters that determine cladding failure conditions, the problem of cladding life control is split into optimization of FE constructional parameters (cladding diameter and thickness; pellet and pellet centre hole diameters; pellet effective density; initial He pressure and grid spacing; etc.) and reactor regime parameters (FE maximum LHR; coolant inlet temperature, pressure and velocity; etc.).
3. CET-method is universal because it is fit for different types of LWR, fuels, fuel claddings, and the cladding failure criterion components do not depend on loading conditions, power maneuvering methods, dispositions of regulating units, FA rearrangement algorithms, etc.
4. Taking into account real FA transposition algorithms, as well as considering a real disposition of control rods, it has been obtained that the AS located between z = 2.19 and 2.63 m is most strained and limits fuel cladding operation time at VVER-1000 day cycle power maneuvering. The fuel pellets corresponding to this limiting AS could be made with holes to increase cladding durability.
5. Taking into account that coolant inlet temperature T_{in} during reactor power maneuvering influences greatly on AO stability, the problem of cladding durability is closely connected to the problem of thermal neutron flux axial distribution stability. The VVER-1000 thermal neutron flux axial distribution can be significantly stabilized at power maneuvering by means of a proper coolant temperature regime assignment. Assuming the maximum divergence between the instant and equilibrium AOs equal to 2%, the regulating unit movement amplitude at constant average coolant temperature $<T>$ is 6%, while the same at constant T_{in} is 4%. Therefore, when using the method with $<T>$=const, a greater regulating unit movement amplitude is needed to guarantee LHR axial stability, than when using the method with T_{in} = const, on the assumption that all other conditions for both the methods are identical. The VVER-1000 average cladding failure parameter after 500 day cycles, for the most strained AS 6, at power maneuvering with $<T>$=const is 8.7% greater than the same with T_{in} = const, on the assumption that AO stability is identical for both the methods.
6. For the VVER-1000 conditions, the rapid creep stage is degenerated when using the zircaloy-4 cladding corrosion models MATPRO-A and EPRI, at the correcting factor COR = - 0.43. This phenomenon proves that it is possible for four years at least, to stay at the steady creep stage, where cladding equivalent creep and radial total strains do not exceed 1-2%, on condition that the corrosion rate is sufficiently small.
7. The VVER-1000 cladding corrosion rate is determined by design constraints for cladding and coolant, and depends slightly on a regime of variable loading. At the same time, practically FE maximum LHR is determined not only by current reactor capacity level, which is a value given to a NPP by the integrated power system, but also by FA rearrangement algorithm. Therefore, the FE cladding rupture life at normal variable loading operation conditions can be controlled by an optimal assignment of coolant temperature regime and FA rearrangement algorithm.

8. The deterministic FA rearrangement efficiency criterion taking into account both safety (cladding durability) and economic (burnup) factors allows us to improve existing methods of fuel rearrangement optimization which take into account only economic efficiency estimated in terms of fuel burnup, power form factor, etc., as well as pin failure probability for a hypothetical severe depressurization accident [17].
9. The probabilistic FA rearrangement efficiency criterion based on Monte Carlo Sampling takes into account robust operation conditions and gives results corresponding to the determinisic ones in principle, though the robust efficiency estimation is more conservative. Hence deterministic FA rearrangement optimization can be used as a preliminary procedure to decrease the number of analysed rearrangement algorithms.
10. CET-method allows us to improve existing control and protection equipment by creating an automized program-technical complex making control of FE cladding durability and optimization of fuel rearrangements in VVER-1000.

Acknowledgements

The authors are indebted to Mr. Motoe Suzuki, Japan Atomic Energy Agency for his consultations about some aspects of use of the FEMAXI code, as well as to Dr. Geoffrey Parks, University of Cambridge for useful discussions about some probabilistic aspects of fuel rearrangement optimization.

References

[1] Pelykh SN, Maksimov MV. Cladding rupture life control methods for a power-cycling WWER-1000 nuclear unit. Nucl. Eng. and Des. 2011; 8: 2956–63.
[2] Kim JH, Lee MH, Choi BK., Jeong YH. Deformation behavior of Zircaloy-4 cladding under cyclic pressurization. Journ. of Nucl. Sci. and Tech. 2007; 44: 1275–80.
[3] Slisenko VI, Mazina NI, Makarovskiy VN, Reshetitskiy SV. Increase of nuclear and radiation safety of the WWR-M research reactor. Odes'kyi Natsional'nyi Politechnichnyi Universytet. Pratsi 2008; 1(29): 112–6 (in Russian).
[4] Maksimov MV, Pelykh SN, Maslov OV, Baskakov VE. Model of cladding failure estimation for a cycling nuclear unit. Nucl. Eng. and Des. 2009; 12: 3021–6.
[5] Suzuki M. Modelling of light-water reactor fuel element behaviour in different loading regimes. Odessa: Astroprint; 2010 (in Russian).
[6] Philimonov PE, Mamichev VV. The "Reactor Simulator" code for modelling of maneuvering WWER-1000 regimes. Atomnaya Energiya 1998; 6: 560–3 (in Russian).
[7] Sosnin OV, Gorev BV, Nikitenko AF. Energy variant of the theory of creep. Novosibirsk: The Siberian branch of the Russian academy of sciences; 1986 (in Russian).
[8] Pelykh SN, Maksimov MV, Baskakov VE. Model of cladding failure estimation under multiple cyclic reactor power changes. In: Proceedings of the 2nd international conference on current problems of nuclear physics and atomic energy, Kiev; 2008. p. 638–41.
[9] Shmelev VD, Dragunov YG, Denisov VP. The WWER active cores for nuclear stations. Moscow: Akademkniga; 2004 (in Russian).
[10] Hohorst J.K. (Ed.). SCDAP/RELAP5/MOD2, Code Manual, Volume 4. MATPRO-A: A Library of Materials Properties for Light Water Reactors Accident Analysis, NUREG/CR-5273, EGG-2555 Vol. 4. Idaho: EG&G; 1990.
[11] Kesterson RL, Yueh HK. Cladding optimization for enhanced performance margins. In: Proceedings of the Int. Conf. TopFuel, Salamanca; 2006.
[12] Pelykh SN, Maksimov MV. Theory of fuel life control methods at Nuclear Power Plants (NPP) with Water-Water Energetic Reactor (WWER). In: Mesquita AZ, editor. Nuclear reactors, Rijeka: InTech; 2012, p. 197–230.
[13] Novikov VV, Medvedev AV, Bogatyr SM. Nuclear fuel operability assurance in maneuver regimes. In: Proceedings of the Int. Ukrainian-Russian Conf. on Experience of the new VVER fuel exploitation, Khmelnitskiy; 2005. p. 1–22 (in Russian).
[14] MATLAB version 7.10.0. Natick: The MathWorks Inc.; 2010.
[15] Vorobyev RY. Albums of neutron-physical characteristics of the reactor core, Unit 5, Zaporizhzhya NPP. Campaigns 20−23. Energodar: Zaporizhzhya NPP; 2008−2011 (in Russian).
[16] Ghisu T, Parks GT, Jarrett JP, Clarkson PJ. Adaptive polynomial chaos for gas turbine compression systems performance analysis. AIAA Journ. 2010; 6: 1156–70.
[17] Parks GT. An intelligent stochastic optimization routine for nuclear fuel cycle design. Nucl. Technol. 1990; 2: 233–46.

Figure captions

Fig. 1. Dependence of SDE on N_{ef} for d_{hole} : 0.140 cm (1); 0.112 cm (2); 0.168 cm (3).

Fig. 2. Dependence of SDE on N_{ef} for UTVS, TVS-A and TVS-W.

Fig. 3. SDE as a function of time for AS 6: (1, 2, 3, 4) at COR = 2, 1, 0, -0.43, respectively; MATPRO-A.

Fig. 4. $\omega(\tau)$ (E-110) and SDE (zircaloy-4) as functions of time: (1) $\omega(\tau)$ according to [13]; (2.1, 2.2) $A(\tau)$ at COR = 0 for the algorithms 55-31-55-55 and 55-31-69-82, respectively; (3.1, 3.2) $A(\tau)$ at COR = 1 for 55-31-55-55 and 55-31-69-82, respectively.

Fig. 5. Disposition of the 10th group: (figure) FA cell number (360 symmetry). The 10-th group cells and the analysed core segment (1/6) borders are in bold.

Fig. 6. Transpositions of FAs during rearrangements: (number) FA cell number; (roman numerals I, II, III and IV) 1st, 2nd, 3rd and 4th campaign year, respectively (6 cells for the 4th year FAs).

Fig. 7. Mean efficiency and standard deviation for $\omega^{\lim}$=13% in the robust case: (number) algorithm number for optimization with 7 cells per year (excluding year 4), A_0=30 MJ/m^3; (pentagon) random algorithm for optimization with 2 cells per year, A_0=40 MJ/m^3.